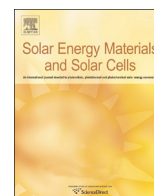




ELSEVIER

Contents lists available at ScienceDirect

Solar Energy Materials & Solar Cells

journal homepage: www.elsevier.com/locate/solmat

Probing the origin of photocurrent in nanoparticulate organic photovoltaics

Natalie P. Holmes^{a,*}, Nicolas Nicolaidis^a, Krishna Feron^{a,b}, Matthew Barr^a, Kerry B. Burke^a, Mohammed Al-Mudhaffer^{a,e}, Prakash Sista^c, A.L. David Kilcoyne^d, Mihaela C. Stefan^c, Xiaojing Zhou^a, Paul C. Dastoor^a, Warwick J. Belcher^a

^a Centre for Organic Electronics, University of Newcastle, University Drive, Callaghan, NSW 2308, Australia

^b CSIRO Energy Technology, Newcastle, NSW 2300, Australia

^c Department of Chemistry, University of Texas at Dallas, 800W Campbell Road BE26, Richardson, TX 75080, USA

^d Advanced Light Source, Lawrence Berkeley National Laboratory, Berkeley, CA 94720, USA

^e Department of Physics, College of Education for Pure Science, University of Basrah, Basrah, Iraq

ARTICLE INFO

Article history:

Received 13 March 2015

Received in revised form

20 April 2015

Accepted 28 April 2015

Keywords:

Morphology

Nanoparticle

Organic photovoltaic

Photocurrent contribution

Scanning transmission X-ray microscopy

ABSTRACT

Varying the donor–acceptor ratio is a common technique in optimising organic photovoltaic (OPV) device performance. Here we fabricate poly(3-hexylthiophene) (P3HT): phenyl C₆₁ butyric acid methyl ester (PCBM) nanoparticle OPVs with varied donor–acceptor ratios from 1:0.5 to 1:2. Device performance increases with PCBM loading from 1:0.5 to 1:1, then surprisingly from 1:1 to 1:2 the performance plateaus, unlike reported trends in bulk heterojunction (BHJ) OPVs where device performance drops significantly as the donor:acceptor ratio increases beyond 1:1. Scanning transmission X-ray microscopy (STXM) measurements reveal core–shell nanoparticles for all donor:acceptor ratios with a systematic increase in the PCBM nanoparticle core volume observed as the PCBM loading is increased. This increases the functional PCBM domain size available for exciton harvesting, contrary to the result observed in BHJ OPV devices where increasing the PCBM loading does not lead to an increase in functional PCBM domains. In addition, STXM measurements reveal that the core–shell nanoparticles have core and shell compositions that change with PCBM loading. In particular, we observe that the PCBM component in the nanoparticle shell phase increases from a concentration that is below the percolation limit to one that is close to the optimal weight fraction for charge transport. This increase in the functional PCBM volume is reflected in an increase in PCBM photocurrent calculated from external quantum efficiency (EQE) measurements.

© 2015 Elsevier B.V. All rights reserved.

1. Introduction

The holy grail of OPV device fabrication is the control of domain morphology to ensure complete exciton separation and efficient charge transport and hence optimum device performance [1–5]. Indeed, different optimal morphologies have been proposed but never successfully implemented due to the complexity of structuring active layers on the nanoscale [5]. As a result the bulk heterojunction (BHJ) structure is now considered as optimal and this architecture by far dominates OPV device studies [6]. Consequently, a judicious choice of additives, solvents and/or fabrication conditions is typically required to engineer indirectly the BHJ active layer morphology [7–11].

* Corresponding author. Tel.: +61 4 1926 6393.

E-mail address: Natalie.Holmes@uon.edu.au (N.P. Holmes).

Varying the donor–acceptor ratio within the active layer is one of the many methods used to optimise BHJ OPV performance [5,9,11–13]. The optimal ratio of P3HT to PCBM in BHJ devices is generally reported to be between 1:1 and 1:0.8 [11], beyond this ratio in either direction performance rapidly drops [13,23,32]. This drop is due to both P3HT being the major contributor to photocurrent and a deterioration in bulk film morphology [13]. Three morphological quantities have been identified as being critically related to the solar cell efficiency of P3HT:PCBM blends: (i) the donor/acceptor domain size, which must be compatible with the exciton diffusion length, (ii) the specific interfacial area, which influences the exciton dissociation rate, and (iii) the percolation pathways, which influence charge carrier transport to the electrodes [12]. Indeed, the prevalence of the BHJ architecture in the literature is driven by the fact that they appear to address all three of these requirements.

In general, P3HT:PCBM OPV devices are fabricated and optimised from the viewpoint that P3HT is the primary exciton generation material with the fullerene acting mainly as an acceptor and electron transport material [14]. As such, optimisation of device performance has focussed upon improvement of the P3HT photoresponse often at the expense of PCBM performance, with the interplay between P3HT crystallisation and fullerene aggregation playing a crucial role [2,15]. In particular, the annealing step that results in P3HT crystallisation, which is essential for efficient hole transport, simultaneously causes PCBM aggregation in the amorphous P3HT interlamellar regions on the > 10–20 nm length scale, with excess PCBM expelled to either the domain boundaries or the surface of the active layer [15]. Consequently, the PCBM in the BHJ architecture contributes very little to total charge generation despite having strong complementary absorption [14].

In the last decade a new materials system for OPVs has been developed, whereby the active layer is fabricated from nanoparticles composed of polymer:fullerene blends [16–20]. Studies of P3HT:PCBM nanoparticles show that a core–shell morphology is adopted, consisting of semicrystalline P3HT-rich shells and PCBM-rich cores [18,21]. Annealing the nanoparticle active layer modifies this initial morphology resulting in retention of the PCBM-rich cores within a matrix of the P3HT-rich shell material [21]. Modelling in these systems has demonstrated that charge transport is not inhibited by this core–shell morphology [22].

In this paper, we constrain the NP core–shell morphology to produce PCBM-rich core and P3HT-rich shell domain dimensions that are comparable to reported exciton diffusion lengths. We observe an increase in PCBM-rich nanoparticle core volume with an increase in PCBM loading; but the entire core volume is still within the exciton diffusion length of the core–shell interface, hence all excitons generated in the PCBM-rich cores can diffuse randomly and undergo dissociation at a core–shell interface. For the 1:2 P3HT:PCBM material feed ratio we do not observe a deterioration in bulk film morphology as reported for BHJ devices [23]. By varying the initial P3HT:PCBM donor:acceptor ratio we are also able to alter the core and shell compositions of the nanoparticles. Consequently, we observe highly efficient harvesting of PCBM generated excitons far in excess of that observed previously for optimised BHJ devices. As such, this work demonstrates that the NP approach delivers a level of control of the mesoscale morphology not possible with conventional BHJ architectures and provides a mechanism via which NP active layer morphologies can be used to outperform conventional BHJ counterparts.

2. Material and methods

2.1. Materials

Poly(3-hexylthiophene) (P3HT) was synthesised via the Grignard metathesis (GRIM) method using the procedure reported previously [21]. Molecular weight was measured by Size Exclusion Chromatography (SEC) analysis on a Viscotek VE 3580 system equipped with Viscogel™ columns (GMHHR-M), connected to a refractive index (RI) detector. GPC solvent/sample module (GPCmax) was used with HPLC grade tetrahydrofuran (THF) as the eluent and calibration was based on polystyrene standards. Running conditions for SEC analysis were flow rate = 1.0 mL/min, injector volume = 100 µL, detector temperature = 30 °C, and column temperature = 35 °C. The polymer sample was dissolved in THF and the solution was filtered through a PTFE filter (0.45 µm) prior to injection. The regioregularity (RR) and the degree of polymerisation (DPn) of the synthesised polymer were determined from the ¹H NMR analysis as described previously [24]. The P3HT material characterisation is detailed in Table 1.

Table 1
P3HT polymer characterisation parameters.

M_n (Da)	M_w (Da)	PDI	DPn	RR
13,290	15,590	1.17	44	98.5

Phenyl C₆₁ butyric acid methyl ester (PCBM) was purchased from Lumtec. Anhydrous chloroform and sodium dodecyl sulphate (SDS) surfactant used for nanoparticle fabrication were purchased from Sigma Aldrich.

2.2. Nanoparticle fabrication

Solutions of P3HT and PCBM in chloroform were prepared in the following ratios 1:0.5 (33 wt% PCBM loading), 1:0.8 (44 wt% PCBM loading), 1:1 (50 wt% PCBM loading), 1:1.2 (55 wt% PCBM loading), 1:1.5 (60 wt% PCBM loading) and 1:2 (67% PCBM loading). These organic phases each had a total solids content of 53.6 mg/ml. Sodium dodecyl sulphate (SDS) was used as the surfactant in the aqueous phase at a concentration of 10.7 mg/ml. The two phases were combined to form miniemulsions and then nanoparticle dispersions according to the method described previously [18]. Nanoparticles fabricated for STXM morphological investigations had a reduced concentration of surfactant in the aqueous phase (0.36 mg/ml) in order to achieve larger particles and a broader distribution in particle sizes for imaging.

2.3. Nanoparticle and nanoparticle film characterisation

Particle size measurements were made by dynamic light scattering (DLS) on a Zetasizer Nano ZS (Malvern Instruments) with a 633 nm laser and a backscatter detector angle of 173°. NP inks were diluted from their original 6 wt% solids content to 0.006 wt% solids using Milli-Q purified water before measurement. Samples were measured at room temperature using disposable plastic cuvettes. A value of 1.33 was used for the refractive index of water and 1.93 for the refractive index of P3HT:PCBM. The refractive index of P3HT:PCBM was determined prior to DLS measurements via optical modelling. The reflectance and transmittance of a solid film along with its thickness were measured, with this experimental information the material was modelled using a set of optical oscillators to accurately model the observed behaviour in the measured film. A total of 10 DLS measurements were performed for each sample, one of these 10 measurements that represents the average has been included in [Supplementary information](#) as a plot of the intensity size distribution for each sample. The Z-average particle diameter was also determined for each sample and is provided in [Supplementary information](#).

For the UV–vis characterisation, the nanoparticle inks were spin coated onto quartz glass slides at the original ink concentration for film measurements. An ultraviolet–visible absorption spectrometer (UV–vis, Varian Cary 6000i) was used to study the absorption of films.

Films were spun at 1750 rpm on quartz for analysis with spectral ellipsometry to match device preparation conditions. A M2000X JA Woollam Spectroscopic Ellipsometer was used to measure the reflection ratio Ψ and phase difference over the wavelength range of 210–1000 nm. The samples were measured using incident angles of 55–75° using 20 revolutions of the analyser per measurement. Optical models were developed by fitting ellipsometry measurements together with transmittance and near normal reflectance measurements using a Varian Cary 6000i UV–vis spectrometer.

Download English Version:

<https://daneshyari.com/en/article/6535223>

Download Persian Version:

<https://daneshyari.com/article/6535223>

[Daneshyari.com](https://daneshyari.com)